Journal of Engineering and Applied Sciences 13 (16): 6713-6718, 2018
ISSN: 1816-949X

The Gas Nitriding Behavior of 31CrMoV9 Grade Steel

[1]Naim Syla, [1]Fisnik Aliaj, [1]Zeqë Tolaj, [2]Naim Mahmudi and [1,3]Arbër Zeqiraj
[1]Department of Physics, Faculty of Mathematics and Natural Sciences, University of Prishtina, Eqrem Cabej Street 51, KS-10030 Prishtina, Kosovo
[2]Department of Physics, Faculty of Natural Science and Mathematics, State University of Tetovo, Bul. Ilinden nn, 1200 Tetovo, Republic of Macedonia
[3]Department of Materials and Metallurgy, Faculty of Geosciences, University of Mitrovica, PIM-Trepca, KS-40000 Mitrovica, Kosovo

Abstract: In this study, the gas nitriding behavior of 31CrMoV9 steel was investigated. The nitriding process was performed in ammonia gas atmosphere at 510°C for 16 and 100 h and 590°C for 4 and 36 h. Optical microscopy was used for examining the morphology of the nitrided layer. Microhardness and compositional depth profiles were obtained using cross-sectional samples. X-ray diffraction method combined with repeated chemical-etching surface layer removal for depth profiling was used to determine the variation of phase composition and residual stress as a function of depth. Optical microscopy examinations of the cross-section of nitrided specimens revealed a two-layer structure of the nitrided zone: compound (or white layer)/diffusion zone. It was found that nitriding for 36 h at 590°C brings about a nitriding zone reaching to a depth of about 700 μm. The highest surface hardness, about 800 $HV_{0.1}$ was obtained for specimens nitrided at 510°C. X-ray diffraction depth profiling confirmed the presence of Fe_3C, CrN, -Fe and residues of • -Fe4N (up to a certain depth) in the diffusion zone. A pronounced dissolution of Fe_3C in the near-surface region and build up towards the nitriding front was observed while CrN nitrides exhibit a more or less constant value across the diffusion zone. All residual stress depth profiles are characterized by a maximum compressive stress occurring at some depth below the specimen surface. Results indicate that the maximum compressive stress decreases with nitriding time and its depth increases with nitriding time due to proceeding homogenization of the specimen, the dissolution of Fe_3C in the near-surface region which is also, supported by overaging of the formed CrN precipitates. Increasing the temperature to 590°C contributed to a diffusion zone with more than 50% lower maximum compressive stress, resulting from the redistribution of carbon in the diffusion layer and faster overaging.

Key words: Gas nitriding, 31CrMoV9 steel, residual stress, X-ray diffraction, diffusion zone, compound layer, vickers hardness

INTRODUCTION

Nitriding is a well-etablished industrial thermochemical surface treatment of iron-based alloys that highly improves mechanical performance with respect to fatigue, tribological behaviour and corrosion (Kolozsvary, 2002; Emami *et al*., 2010; Jegou *et al*., 2011; Altinsoy *et al*., 2014). The nitriding process invloves the diffusion of atomic nitrogen which is accompanied by a hardening effect combined to compressive residual stresses. These effects find its origin in the volume changes during nitrogen diffusion such as lattice distorsions and differences in the molar volumes between alloy nitride precipitates and the ferrite matrix (Wiggen *et al*., 1985; Jegou *et al*., 2011; Fallot *et al*., 2014; Kang *et al*., 2016; Syla *et al*., 2017). The gas nitriding is one of the most versatile nitriding processes with many advantages over the liquid and plasma nitriding. A precise process control of nitrogen uptake via the thermodynamic chemical potential of nitrogen in the gas phase is the main advantage of the gas nitriding method. Controlling the nitriding process with a thermodynamic parameter makes it possible to produce nitriding layers that meet various technological requirements (Korwin *et al*., 2004).

Kang *et al*. (2016) have studied the influence of nitriding parameters (time and nitriding potential) on the microstructure evolution of 31CrMoV9 grade steel during controlled gaseous nitriding treatment. A graded microstructure developed upon nitriding of 31CrMoV9

Corresponding Author: Arbër Zeqiraj, Department of Materials and Metallurgy, Faculty of Geosciences, University of Mitrovica, PIM-trepca, KS-40000 Mitrovica, Kosovo

steel dependent on nitriding potential and nitriding time which had pronounced consequences in the evolution of residual stress and hardness. Emami *et al.* (2010) studied the high temperature tribological behavior of 31CrMoV9 gas nitrided steel and found that the wear resistance of the nitrided steel improved many-folds compared to the untreated specimens due to formation of smooth and compacted protective tribological layers. Celebi Efe investigated the growth kinetics of nitrided layer of the gas nitrided 31CrMoV9 steel. The diffusion coefficients and activation energy for the diffusion of nitrogen in 31CrMoV9 steel matrix were evaluated using common fitting procedures applied to the experimentally acquired thickness data. In our recent paper (Syla *et al.*, 2016), we have used a new and intuitive approach to study the growth kinetics of nitrided layer of the gas nitrided 31CrMoV9 grade steel. The procedure led to the determination of activation parameters for the diffusion of nitrogen in the steel matrix and to the reduction of errors because it only requires one-time regression to evaluate the data. The present work aims to work out the relationship between the nitriding parameters, the microstructure and the resulting stress and hardness distribution of the gas nitridied 31CrMoV9 steel.

MATERIALS AND METHODS

Chemical composition of 31CrMoV9 steel was analyzed using the spark emission spectroscopy (Jobin Yvon make, model JY-132F) and the results are given in Table 1. The contents of carbon and other alloying elements are consistent with the requirements of the DIN standard 17211. The steel specimens were disk-shaped with dimensions of Ø35×10 mm. The surfaces of the substrates were mechanically ground on SiC paper of successively finer grades, starting with 320-grit and proceeding to 400 and 600-grit paper, using water to keep the specimens cool. Before gas nitriding treatment, the microstructure of the original steel specimens was reestablished by thermal treatment. The details of this treatment are reported in our earlier paper (Syla *et al.*, 2016). The gas nitriding was performed in air doped ammonia atmosphere at 510°C (for 16 and 100 h) and 590°C (for 4 and 36 h). Parameters of the nitriding treatment were selected such that the nitriding potentials were 3.4 and 2.82 $atm^{-1/2}$ at temperatures of 510 and 590°C, respectively, providing for the same nitrogen concentration at the surface of the steel specimens.

A series of experiments was performed to investigate the nitrided specimens. For this purpose, the samples were cut into several pieces which were then used for different analyses.

Phase depth distribution in the nitrided layers was determined by performing X-Ray Diffraction (XRD) measurements combined with repeated surface layer removals with a certain thickness. The measurements were carried out with Co-K• radiation by using a Seifert-FPM URD63 diffractometer in a conventional •/2• Bragg-Brentano geometry. The surface layers were removed (in steps of 20-80 μm) by controlled etching to exhibit deeper areas of the nitrided zone which allowed XRD phase determination of the occurring surfaces. Residual stress analysis was also, performed after each layer removal. The measurements were carried out by laboratory X-ray diffraction using a Huber diffractometer with Cr-K• radiation on the {211} diffraction plane of •-Fe. The $\sin^2$• method was used (Noyan and Cohen, 1987), assuming a macroscopically elastically isotropic specimen with a plane, rotationally symmetric biaxial stress state.

Table 1: Chemical composition (in wt.%) of 31CrMoV9 steel. The difference to 100 wt.% is Fe

Chemical	Values
C	0.29(1)
Cr	2.17(2)
Mn	0.70(1)
V	0.15(1)
Mo	0.27(1)
Si	0.26(1)
S	0.004(1)
P	0.016(2)
Al	0.022(2)

For optical microscopy examinations, hardness measurements according to Vickers and nitrogen depth profiling with Electron Probe Microanalysis (EPMA), a cross-sectional metallographic preparation of the nitrided steel specimens was conducted. The procedure consisted in cutting the specimens to obtain a cross-section, mounting in resin, followed by grinding and polishing steps in the final step with 1 μm grains. To avoid damaging and rounding off at the edges upon cross-sectional preparation, the specimens were protected by Ni-plating before mounting in resin. Hardness measurements were performed on polished cross-sections of nitrided specimens by using a PCE Leco microhardness tester under a load of 0.9807 N ($HV_{0.1}$) and a dwelling time of 10 sec. For metallographic examinations with the optical microscope, the nitrided specimens were etched in a 2% Nital solution. Nitrogen concentration-depth profiles were determined with EPMA technique by using a Joel JXA-8900 RL microanalyser operated at 20 kV. EPMA measurements were performed on a polished cross-section of the nitrided specimens, perpendicular to the surface, starting at the surface and moving in 5 μm increments towards the depth of the specimens.

RESULTS AND DISCUSSION

Morphology and thickness of nitrided layers: Figure 1 shows light optical micrographs of the specimen nitrided at 590°C for 36 h which is representative of all the

Table 2: Variation with nitriding time and temperature of the compound layer thickness, diffusion layer thickness, surface hardness, case depth, maximum compressive stress and depth of maximum stress

Nitriding temperature (°C)	Nitriding time (h)	Compound layer thickness (μm)	Diffusion layer thickness (μm)	Surface hardness (HV)	Case depth, CD (μm)	Maximum compressive stress (Mpa)	Depth of maximum stress (μm)
510	16	10.1	245	770	305	-840	50
	100	14.3	619	788	620	-530	80
590	4	19.5	239	744	280	-340	60
	36	32.0	654	602	700	-250	300

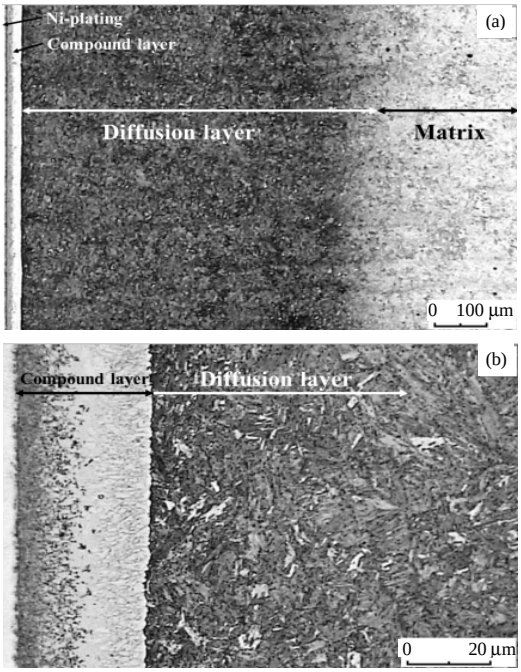

Fig. 1: Light optical micrograph of 31CrMoV9 steel specimen nitrided at 590°C for 36 h. The entire nitrided zone (compound and diffusion zone) and the un-nitrided core (matrix) is shown in: a) An enlarged portion of the outer edge region of the specimen is shown in and b) The first layer visible in the micrographs is due to Ni-plating which was introduced to reduce damaging at the edges during metallographic preparation

samples. Evidently there are three distinct layers on the cross-section of a nitrided specimen: the outermost layer which is generally referred to as the compound layer or white layer, the internal diffusion layer underneath the compound layer and the un-nitrided core (matrix). The compound layer consists of dense and fine precipitates of iron nitrides and on the surface shows a pore space which is formed by the recombination of nitrogen atoms. The observation of porous structure in the compound layer is consistent with the development of porosity in a model Fe-Cr-C alloy steel (Jegou *et al*., 2011) (with Cr and C content similar to 31CrMoV9 steel) during nitriding under conditions similar to this work. In the diffusion zone, nitrogen is mainly incorporated into the existing iron lattice as interstitial atoms or as finely dispersed alloy nitride precipitates.

The layer thicknesses, listed in Table 2 were determined using the optical micrographs. At each temperature, the thickness of the compound and diffusion layer both increase with increasing nitriding time which is an expected result as increased time provides more atomic nitrogen diffusion towards the core. The thickness and composition of layers that develop during the nitriding process are affected by the type of chemical reactions occurring at the sample surface, the diffusivity of nitrogen in the treated material, the gas mixture ratio, the process temperature and time.

Composition and microhardness: Nitrogen concentration-depth profiles of nitrided 31CrMoV9 steel specimens are shown in Fig. 2. The diagrams show the increasing penetration depth of nitrogen with increasing nitriding time. An increased time provides more atomic nitrogen diffusion towards the core while the increasing temperature raises the diffusivity of nitrogen, providing for the same effect. The increase in diffusivity of nitrogen with increasing temperature can be seen in that approximately the same penetration depths are achieved with shorter nitriding times. Nitriding for 36 h at 590°C brings about a diffusion zone reaching to a depth of about 700 μm.

Microhardness-depth profiles obtained from cross-sections of nitrided specimens are also, shown in Fig. 2 superimposed to nitrogen concentration-depth profiles. Evidently, the microhardness-depth profiles resemble the same characteristics as the nitrogen concentration-depth profiles. It is observed that the hardness of the nitrided layer is much higher than that of the core due to formation of hard iron and chromium nitrides in the nitriding layer (as determined by the XRD analysis). All hardness-depth profiles end up at the level of the core hardness which is about 290 $HV_{0.1}$.

The observed decrease in hardness with depth is due to decrease of nitrogen concentration. The highest surface hardness of about 800 $HV_{0.1}$ was obtained for specimens nitrided at 510°C. At this temperature, the

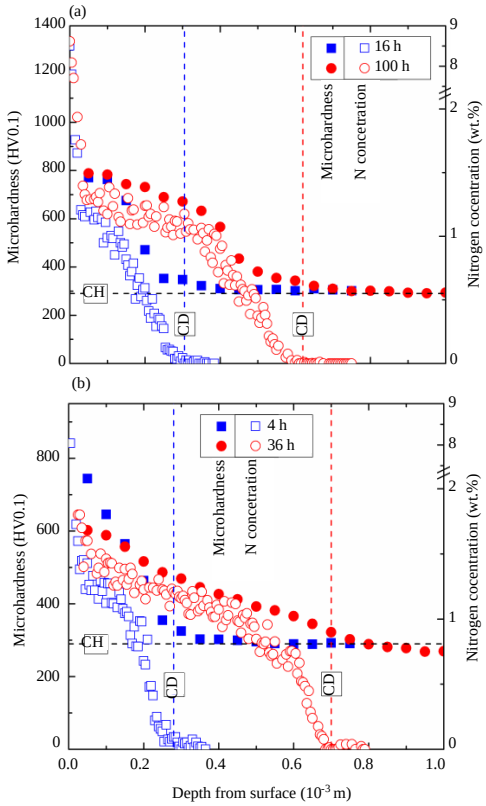

Fig. 2: Microhardness-and N concentration-depth profiles of 31CrMoV9 steel specimens nitrided at; a) 510°C and b) 590°C. CH represents the core hardness level; CD represents the case depth for the particular nitriding times

surface hardness also, remains almost constant despite the considerable increase in the nitriding time from 16-100 h. The surface hardness decreases when increasing the temperature to 590°C. At this temperature, the surface hardness is reduced by about 140 $HV_{0.1}$ when increasing nitriding time from 4-36 h. The cause of hardness drop is presumably relaxation processes in the layers. The values of surface hardness and case depth, calculated according to the DIN standard 50190-3 are given in Table 2.

Phase distribution in the diffusion layer: The qualitative and quantitative phase depth-dependent measurements were carried out over the entire diffusion zone. Fig. 3 shows a typical X-ray diffraction pattern recorded after the fourth subsequent surface layer removal of the specimen nitrided at 590°C for 36 h and clearly shows peaks of •-Fe (ferrite), CrN and Fe_3C (cementite), indicated for better readability. Figure 4 shows the phase depth distribution of the main components, •-Fe_4N,CrN and

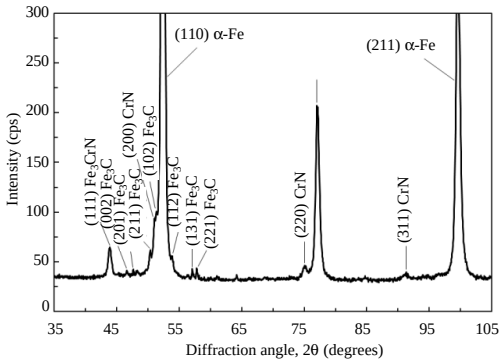

Fig. 3: X-ray diffraction pattern of 31CrMoV9 steel specimen nitrided at 590°C for 36 h after the fourth layer removal. The diffraction pattern is collected with Co-K• radiation

Fe_3C determined from integral intensities of the diffraction patterns, the difference to 100 wt.% consists mainly of •-Fe. The first measurement points refer to the beginning of the diffusion zone after removal of the compound layer. Residues of • nitride are still visible up to a depth of about 40 μm at 590°C/4 h and 170 μm at 590°C/36 h. It is suggested that the • nitride preferentially grows along grain boundaries (and presumably pores that develop during nitriding) in the diffusion zone (Jegou *et al*., 2011).

Phase analysis shows a dissolution of Fe_3C in the part of the diffusion zone close to the compound layer, which combined with the formation of porosity along grain boundaries, provide a means for stress relaxation. Towards the nitriding front, an accumulation of Fe_3C is observed which is presumably the stress-induced precipitation of Fe_3C. The course of CrN phase is interesting in the longer nitriding time. The CrN content, apart from a small deviation down to almost the end of the diffusion zone is at a level of about 3 wt.%. At the shorter time, an even CrN content is also, present up to about 200 μm. Only then will it decline to zero.

Residual stress: Residual stress distributions after 16 and 100 h of nitriding at 510°C and 4 and 36 h of nitriding at 590°C are shown in Fig. 5. Evidently, all profiles are characterized by a maximum compressive stress occurring at some depth below the surface and a subsequent decrease with increasing depth until a more or less constant stress of small tensile value occurs in the region of the un-nitrided core adjacent to the nitrided zone. Table 2 lists the maximum compressive stress values and depth of their occurrence. During nitriding of 31CrMoV9 steel, nitrogen dissolves in the ferrite matrix and forms alloy element nitrides (CrN as revealed by XRD). The

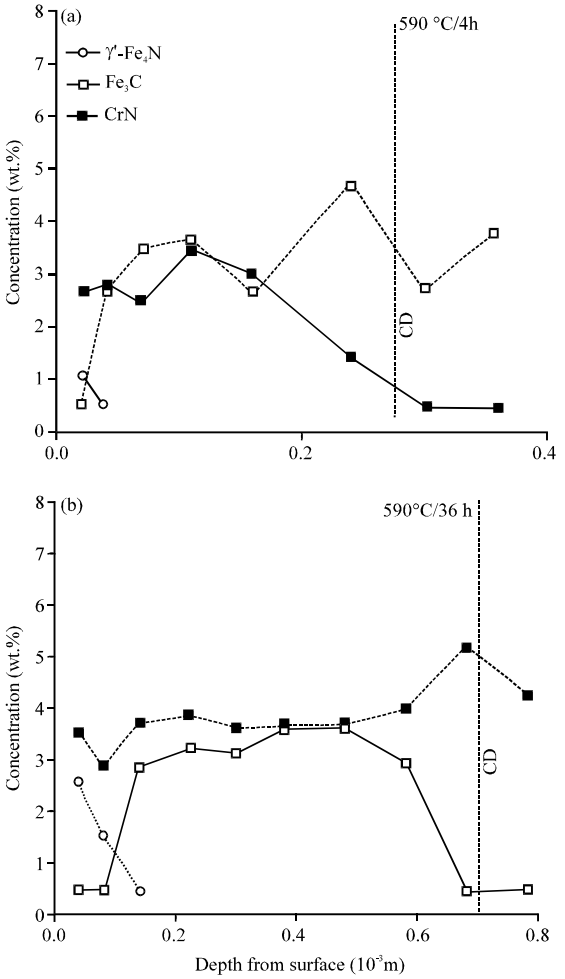

Fig. 4: Phase distribution of main components in the diffusion zone of 31CrMoV9 steel nitrided at: a) 590°C for 4 h and b) 590°C for 36 h. The first measurement points refer to the beginning of the diffusion zone after removal of the compound layer. CD represents the case depth

precipitation of CrN particles leads to an expansion of the nitrided zone due to the volumetric mismatch between the ferrite and CrN lattices. As a result of self-equilibrating stress state and because the nitrided zone and the un-nitrided core are attached to one another, a compressive residual stress must develop in the nitrided zone. The mechanical equilibrium between the nitrided zone and the un-nitrided core requires the development of small tensile stress in the (larger) un-nitrided core.

Results also, indicate that the value of the maximum compressive stress decreases with nitriding time and its depth increases with nitriding time, consistent with Jegou *et al.* (2011). The decrease of residual stress upon continued nitriding is the consequence of the

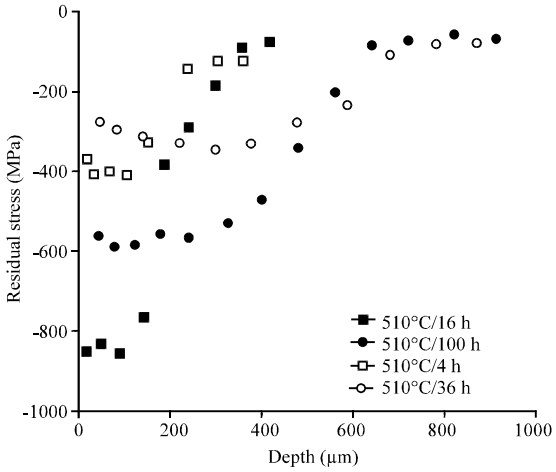

Fig. 5: Residual stress-depth profiles of 31CrMoV9 steel nitrided at 510 and 590°C for various nitriding times

proceeding homogenization of the specimen, the pronounced dissolution of cementite in the near-surface region (as shown in Fig. 4) which is also, supported by overaging of the formed CrN precipitates. The formation of •'-Fe_4N nitrides along grain boundaries in the diffusion zone is also, likely to be associated with a contribution to stress. The increase of nitriding temperature contributes to a diffusion zone with more than 50% lower maximum compressive stress, resulting from the redistribution of carbon in the diffusion layer and faster overaging.

When comparing the residual stress-depth profiles with the respective hardness-depth profiles no direct relationship is visible. At 510°C, the residual stress level at the surface relaxes by an amount of 300 MPa with increasing nitriding time but this significant drop is not reflected in the hardness values were for both nitriding times a high surface hardness of ~800 $HV_{0.1}$ is observed. Furthermore it can be seen that the stress level of the long nitriding time decreases almost continuously from the surface to the core whereas the hardness initially does not go down so, strongly and only drops steeply starting at ~400 µm (Fig. 2a). Although these phenomena are not so, pronounced at 590°C it can nevertheless be assumed that the stress level is independent of the layer hardness. This is entirely understandable, since, for example with a fully nitrided sample the residual stress is zero but the hardness can be very high.

CONCLUSION

The aim of this study was to work out the relationship between the nitriding parameters, the microstructure and he resulting stress and hardness

distribution of the gas nitridied 31CrMoV9 grade steel. A wide range of classical methods was used to investigate the nitriding samples. In addition, to microstructural analysis by optical microscopy, the nitriding samples were characterized by nitrogen-and hardness-depth curves. X-ray diffraction methods for the measurement of residual stress distribution and for qualitative and quantitative phase analysis also, played an important role. The nitriding layer thickness could be measured successfully using metallographically prepared cross-sections. It was found that nitriding times were favorably chosen for achieving similar layer thicknesses at the two investigated temperatures. The hardness-depth profiles of the nitriding layers showed increasing nitriding depths as expected during longer nitriding periods, although, the gradients have a different shape. The phase analysis shows decarburization in the near-surface region and a constant CrN content from the beginning. Maximum compressive stress of about 800 MPa at 510°C/16 h is achieved directly at the surface. At 590°C, the maximum is due to the decarburization further inside. There was no correlation between residual stress and hardness. Despite a stress relaxation of about 300 MPa between 16 and 100 h of nitriding at 510°C, both states have the same hardness.

REFERENCES

Altinsoy, I., K.G. Onder, F.G.C. Efe and C. Bindal, 2014. Gas nitriding behaviour of 34CrAlNi8 nitriding steel. Acta Phys. Pol. A., 125: 414-416.

Emami, M., H.M. Ghasemi and J. Rassizadehghani, 2010. High temperature tribological behaviour of 31CrMoV9 gas nitrided steel. Surf. Eng., 26: 168-172.

Fallot, G., S. Jegou and L. Barrallier, 2014. Evolution of residual stresses during short time nitriding of 33CrMoV12-9 steel grade Adv. Mater. Res., 996: 544-549.

Jegou, S., L. Barrallier and R. Kubler, 2010. Phase transformations and induced volume changes in a nitrided ternary Fe–3% Cr–0.345% C alloy. Acta Mater., 58: 2666-2676.

Jegou, S., L. Barrallier, R. Kubler and M.A. Somers, 2011. Evolution of residual stress in the diffusion zone of a model Fe-Cr-C alloy during nitriding. J.Heat Treat. Mater., 66: 135-142.

Kang, C.W., S.R. Meka, T. Steiner, R.E. Schacherl and E.J. M ittemeijer, 2016. Microstructural evolution of 31CrMoV9 steel upon controlled gaseous nitriding treatment. J. Heat Treat. Mater., 71: 181-190.

Kolozsvary, Z., S.A.S.C. Plasmaterm and R. Tg-Mures, 2002. Residual Stresses in Nitriding. In: Handbook of Residual Stress and Deformation of Steel, Totten, G., M. Howes and T. Inoue (Eds.). ASM International, Geauga County, Ohio, pp: 209-219.

Korwin, M.J., C.D. Morawski, W.K. Liliental and G.J. Tymowski, 2004. Design of Nitrided and Nitrocarburized Materials. In: Handbook of Metallurgical Process Design, Xie, L., K. Funatani and G.E. Totten (Eds.). Marcel Dekker Inc., New York, USA., pp: 545-590.

Noyan, I.C. and J. B. Cohen, 1987. Residual Stress, Measurement by Diffraction and Interpretation. Springer-Verlag, New York, 1987.

Syla, N., F. Aliaj and B. Dalipi, 2016. The law of growth of nitrided layer in 31CrMoV9 steel. Acta Phys. Polonica A., 130: 83-86.

Syla, N., F. Aliaj and M. Rama, 2017. Hardness curves for 31CrMoV9 steel after gas nitriding. Acta Phys. Pol. A., 132: 484-486.

Wiggen, P.C., H.C.F. Rozendaal and E.J. Mittemeijer, 1985. The nitriding behaviour of iron-chromium-carbon salloys. J. Mater. Sci. 20:4561-4582.